Quaternary Science Reviews 258 (2021) 106869

Contents lists available at ScienceDirect

Quaternary Science Reviews

journal homepage: www.elsevier.com/locate/quascirev

Human influence on the continental Si budget during the last 4300 years: $\delta^{30}Si_{diatom}$ in varved lake sediments (Tiefer See, NE Germany)

Carla K.M. Nantke [a, *], Achim Brauer [b, c], Patrick J. Frings [d], Markus Czymzik [e], Thomas Hübener [f], Johanna Stadmark [a], Olaf Dellwig [e], Patricia Roeser [e], Daniel J. Conley [a]

[a] Lund University, Department of Geology, Lund, Sweden
[b] German Research Centre for Geosciences (GFZ), 4.3 Climate Dynamics and Landscape Evolution, Potsdam, Germany
[c] University of Potsdam, Institute of Geosciences, Potsdam, Germany
[d] German Research Centre for Geosciences (GFZ), 3.3 Earth Surface Geochemistry, Potsdam, Germany
[e] Leibniz Institute for Baltic Sea Research Warnemünde (IOW), Marine Geology, Rostock, Germany
[f] University of Rostock, Institute of Biosciences, Department of Botany and Botanical Garden, Rostock, Germany

ARTICLE INFO

Article history:
Received 4 October 2020
Received in revised form
16 February 2021
Accepted 22 February 2021
Available online xxx

Handling Editor: P Rioual

Keywords:
Diatoms
Human impact
Lake sediments
Si isotopes
Soil Si

ABSTRACT

The continental silicon (Si) cycle, including terrestrial and freshwater ecosystems (lakes, rivers, estuaries), acts as a filter and modulates the amount of Si transported to the oceans. In order to link the variation in the terrestrial Si cycle to aquatic ecosystems, knowledge on changes in vegetation cover, soil disturbance and the impact of human activity are required. This study on varved lake sediments from Tiefer See near Klocksin (TSK) in northeastern Germany investigates Si isotope variations in diatom frustules ($\delta^{30}Si_{diatom}$) over the last ~4300 years. $\delta^{30}Si_{diatom}$ values vary between 0.37 and 1.63‰. The isotopic signal measured in centric (mostly planktonic) and pennate (mostly benthic) diatoms shows the same trend through most of the record. A decrease in $\delta^{30}Si_{diatom}$ coinciding with early deforestation between 3900 and 750 a BP in the catchment area, points to an enhanced export of isotopically light dissolved silica (DSi) from adjacent soils to the lake. The burial flux of biogenic silica (BSi) observed in the lake sediments increases with cultivation due to enhanced nutrient supply (N, P and Si) from the watershed and nutrient redistribution caused by wind-driven increased water circulation. When the cultivation intensifies, we observe a shift to higher $\delta^{30}Si_{diatom}$ values that we interpret to reflect a diminished Si soil pool and the preferential removal of the lighter ^{28}Si by crop harvesting. Human activity influences the DSi supply from the catchment and appears to be the primary driver controlling the Si budget in TSK. Our data shows how land use triggers variations in continental Si cycling on centennial timescales and provides important information on the underlying processes.

1. Introduction

On geological timescales the sequestration of carbon via weathering of silicate rocks regulates atmospheric CO_2 concentrations (Walker et al., 1981) and represents the starting point in the global Si cycle. A growing number of studies have also documented the importance of quantifying annual to centennial changes in continental Si fluxes by investigating environmental factors that influence the Si cycle on a regional scale (Barão et al., 2015; Struyf et al., 2010; Vandevenne et al., 2015). Short term changes of Si budgets in terrestrial ecosystems hold the potential to control Si fluxes to the ocean and therefore the global Si cycle. Since the annual fixation of dissolved Si (DSi) as biogenic Si (BSi) in the vegetation and its release to the soil pool can be several orders of magnitude greater than Si release from mineral weathering, terrestrial ecosystems (including terrestrial vegetation, pedosphere, aquatic freshwater systems) act as a 'filter' between Si export from the lithosphere and the ultimate Si transport to the oceans (Dürr et al., 2011; Struyf and Conley, 2011). Variation in DSi concentrations influence phytoplankton community composition - in particular diatom abundances - and therefore the rate of carbon sequestration. Changes in vegetation due to climate variability, ecosystem succession, or human activity can alter the uptake and recycling of Si in terrestrial ecosystems (Cornelis et al., 2011). In

* Corresponding author.
E-mail address: carla.nantke@geol.lu.se (C.K.M. Nantke).

https://doi.org/10.1016/j.quascirev.2021.106869

particular, increasing land cultivation can potentially change the capacity of the terrestrial Si filter (Clymans et al., 2011). However, the dominant processes and their contribution to the global Si budget on a range of timescales remain poorly constrained.

The functioning of the terrestrial Si filter is locally determined by biodiversity, hydrology and lithology (Struyf and Conley, 2011). On geologically short time scales (decades to centuries), Si recycling in soils and the utilization of DSi by plants create a so-called "terrestrial loop" in the vegetation-soil system: DSi is taken up from soil solutions by higher plants and fixed as phytoliths (hydrated amorphous SiO_2 particles). After litterfall or plant death, the Si returns to the soil system, where it either dissolves, producing DSi, or contributes to replenish the soil amorphous Si (ASi), a pool which also includes phases of pedogenic origin (clay-sized Si minerals). These clay-sized secondary phases can (re)dissolve and supply DSi to the soil system. However, their contribution differs depending on physico-chemical conditions determining the rate of particle dissolution in soil waters (Cornelis and Delvaux, 2016).

Human interferences to the Si cycle, including deforestation, the plowing of soils, or intensive fertilizer use can impact the terrestrial Si loop. Changes in vegetation cover that influence the Si pool in plants (phytoliths) and soils (ASi), or the fluxes between them, have been shown to alter the Si budget at local to regional scales (Clymans et al., 2011; Conley et al., 2008; Vandevenne et al., 2012). Compared to undisturbed environments, it is assumed that cultivated landscapes export larger amounts of DSi during relatively short time periods (decades) until a lower steady-state soil pool of ASi is achieved (Clymans et al., 2011; Struyf et al., 2010). The depletion of Si in the soil ASi pool has implications for downstream ecosystems and the long-term sustainability of cultivated landscapes. Yet, the lack of river chemistry data over decadal-centennial timescales makes the above assumptions difficult to test.

Clymans et al. (2011) used a chronosequence approach to compare the storage of ASi in temperate soils along a human impact gradient in southern Sweden. Based on measured soil ASi inventories of about 67,000 kg SiO_2 ha^{-1} in an undisturbed forest site, and ~27,000 kg SiO_2 ha^{-1} in cultivated landscapes, they estimated a reduction in the global soil ASi pool by about 10% since 4950 a BP, based on expanding area of land used for agriculture. Distributed globally over this time, this would be equivalent to about 20% of the annual DSi flux transported by rivers to the ocean. Vandevenne et al. (2015) further revealed an increase in silicon isotope ratios in soil-water DSi ($\delta^{30}Si_{DSi}$) along a land use gradient, as the Si taken from soil pools by crop harvest preferentially removes the lighter Si isotopes. These studies provided clear evidence that human activity can substantially and rapidly impact the pools and fluxes that comprise the terrestrial Si cycle. To provide a longer-timescale perspective, Nantke et al. (2019) used a sediment record to investigate the Si budget of the Chesapeake Bay estuary (northeastern United States) through the Holocene. They demonstrate the impact of catchment land use changes on the Si budget of the estuary since European settlement ~250 a BP. However, Chesapeake Bay's large watershed (166,000 km^2) with heterogeneous soils and a relatively short period of large-scale (post-European settlement) human impact (ca. 320 years) led to a superposition of simultaneously occurring processes (including deforestation, changing nutrient inputs, damming and agriculture). This made a clear distinction of individual influences on the regional Si cycle challenging. To improve our mechanistic understanding of continental Si cycling, we investigate here the varved sediment record of Tiefer See in northeastern Germany covering the last 4300 years. Its relatively small catchment area (5.5 km^2) and well-dated sediment record of local human activity (Dräger et al., 2017) provide suitable conditions to investigate the importance of land use and vegetation changes for the continental Si cycle through time. Additionally, a wealth of environmental proxy records from Tiefer See allows us to identify and distinguish various influences on the Si fluxes (Dräger et al., 2019).

The main aim of this study is to reconstruct and quantify changes in Si cycling in the Tiefer See catchment and their driving factors. We focus on the use of Si isotopes in diatom frustules (expressed as $\delta^{30}Si_{diatom}$) preserved in the lake sediments, supplemented with a comprehensive multi-proxy dataset including major element contents, macrofossil analysis, diatom assemblage composition and pollen counts from the same archive (Dräger et al., 2017; Kienel et al., 2013; Theuerkauf et al., 2015). The $\delta^{30}Si_{diatom}$ is controlled by two main parameters: 1) $\delta^{30}Si$ of the ambient water ($\delta^{30}Si_{DSi}$) during diatom growth and 2) the relative amount of DSi utilization, i.e. the ratio of lake internal biogenic silica (BSi) production to catchment DSi supply. This second parameter represents a mass-balance control on the expression of Si isotope fractionation. Both factors are, in turn, influenced by environmental conditions (Nantke et al., 2019). A third parameter, the magnitude of Si isotope fractionation factor by diatoms, is considered as a constant value, independent of species composition (Alleman et al., 2005). This allows us to investigate how both the Si import and Si uptake have evolved in the Tiefer See ecosystem, including the lake and its catchment.

We generate Si isotope records from hand-picked planktonic (centric taxa, $\delta^{30}Si_{centr}$) and benthic (pennate taxa, $\delta^{30}Si_{penn}$) diatom species that allow us to differentiate changes in Si fluxes in different water layers with their specific conditions. Comprehensive monitoring of Tiefer See waters and modern sedimentation since 2012 provides a characterization of the lake system as basis for our paleo-interpretations (Roeser et al., 2021).

2. Study site

Tiefer See (TSK = Tiefer See Klocksin, 53°35.5′N, 12°31.8′E) is located in northeastern Germany as a part of the Klocksin lake chain, which formed as a sub-glacial channel system during the last glacial maximum with water flow from north to south (Fig. 1). The connections to its adjacent lakes, Flacher See (FS, the northern inlet) and Hof See (HS, the southern outlet), depend primarily on the lake level and seasonality. Today the outlet to HS is interrupted and the inlet from FS is intermittent, consisting of only isolated water pools in the transition area between the lakes. The lake has a surface area of 0.75 km^2 and a maximum water depth of 62 m (Czymzik et al., 2015; Kienel et al., 2013). The relatively small 5.5 km^2 catchment area is covered by glacial till and consist of a heterogenous mix of clay minerals, limestone and sand. Mean monthly temperatures vary between 0 °C in January and 18 °C in July. A precipitation maximum occurs during summer (mean annual precipitation = 560 mm)(Dräger et al., 2017).

Modern land use in the watershed is dominated by crop cultivation (46.7%), grassland (14.9%) and forest (21.5%) (Theuerkauf et al., 2015). However, Theuerkauf et al. (2015) also showed that landscape management has caused frequent changes in plant abundance and vegetation openness even within the last decade. The lake is mono- or dimictic, depending also on the formation of ice cover during winter (Dräger et al., 2019). Overturning events can differ in strength and duration, directly controlling lake internal sediment resuspension, as well as nutrient and oxygen distribution within the water column. A diatom dominated phytoplankton production peak occurs in late spring/early summer (Kienel et al., 2013). However, sediment trap material and a second DSi minima in the epilimnion, e.g. between 0.15 and 0.81 mg SiO_2 L^{-1} in Oct/Nov 2015, suggest that in modern times diatom blooms also occur in autumn, dominated by pennate diatoms (Roeser et al., 2021).

The TSK sediments record the development of the lake and

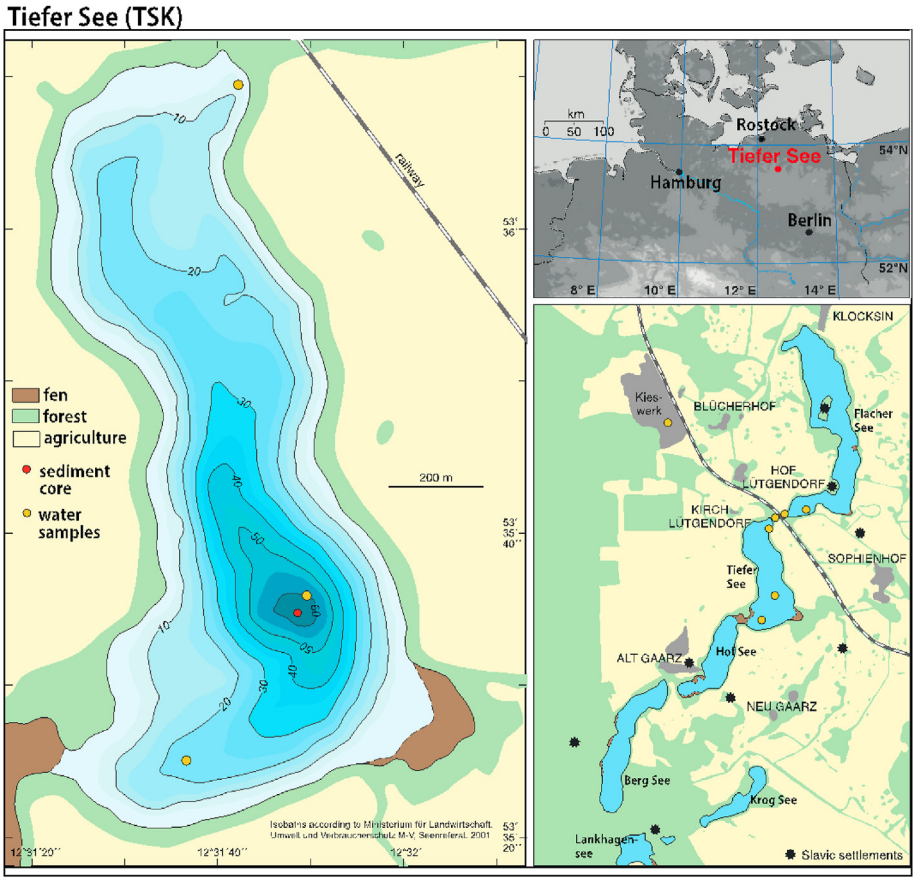

Fig. 1. Bathymetric map of Tiefer See and its location in the Klocksin Lake Chain with sampling and coring locations. Historic Slavic settlements are marked as stars. Modified after (Dräger et al., 2017).

catchment during the Holocene (Dräger et al, 2017, 2019). Alternating varved and non-varved (homogenous) sediment sections reflect anoxic and oxic bottom water conditions, respectively, that have been interpreted in terms of changing climate, vegetation and land use in the catchment (Dräger et al., 2017; Kienel et al., 2013). The detrital mineral assemblage in the TSK sediments comprises mainly quartz (up to 25 w%) and minor amounts of rutile (~1–1.5 w %). Aside these minerals, some authigenic carbonates and pyrite were identified in the sediments. The varve composition varies through the sediment core. Modern varves from the last decade consist of three sub-layers: a planktonic diatom sub-layer, followed by a summer calcite sub-layer, followed by a sub-layer of resuspended sediments (Roeser et al., 2021). In addition, varves from the last century can hold up to five sub-layers: a planktonic diatom layer, a mixed layer, a calcite layer, an organic layer, and a mixed autumn layer (Dräger et al., 2017). Human colonization in northeastern Germany is evidenced since at least the early Mesolithic (~12,000 a BP), with increasing population density, deforestation and intensifying landscape cultivation occurring in the second half of the Holocene (Kappler et al., 2018). As indicated by pollen assemblages, large-scale human activity in the catchment of TSK started around 4000 a BP and shows different periods of deforestation and the cultivation of crops (Theuerkauf et al., 2015). Low lake levels throughout the whole research period led to a disconnection from its adjacent lakes. Thus, $\delta^{30}Si_{DSi}$ is assumed to be determined by Si inputs from the catchment, groundwater and redissolving BSi before and after deposition. With the construction of a railroad track in the 1880s the natural connection between TSK and FS became an artificial channel.

3. Methods

3.1. Water samples

Physical and chemical parameters (e.g. temperature, pH, oxygen content) in the water column were measured at TSK using a multiparameter water quality probe (YSI 6600 V2) at 1 m intervals throughout the entire water column, with an average daily resolution in an ongoing monitoring program since May 2012.

Water samples from TSK were collected at monthly resolution between January and December 2019. Six water samples were taken along a depth profile (0, 7, 17, 25, 35 and 45 m water depth) at the central sampling station (Fig. 1). Additional surface water samples were taken in the lake near the main inlet and outlet, as well as from the main inlet itself, i.e. the artificial connection between TSK and FS (February to December 2019) (Fig. 1). All water samples were filtered through 0.45 μm Nucleopore filters, acidified with HCl to approximately pH 2 immediately after collection and stored in a refrigerator at ~4 °C. DSi concentrations in all water samples were analyzed with a SmartChem 200 discrete chemical analyzer using the molybdate-blue methodology (Conley and Schelske, 2001; Strickland and Parsons, 1972).

3.2. Sediment samples

3.2.1. Sediment core and age model

Seven parallel sediment cores consisting of 2 m long segments were retrieved from the deepest part of TSK in 2011 and 2013 (TSK11 & TSK13). A continuous composite profile was constructed

through core-to-core correlation of macroscopic lithological layers (Dräger et al., 2017). The published age model is based on varve counting, tephra layers and AMS ^{14}C dates (Dräger et al., 2017; Wulf et al., 2016). For this study, 120 sediment samples covering the last ~4300 years were extracted from the composite profile with a resolution of 2 cm until 159 a BP, 5 cm from 897 to 159 a BP, 10 cm from 2164 to 897 a BP and 5 cm from 4235 to 2164 a BP. This sampling strategy was chosen to increase the data resolution during periods of major vegetation changes, as indicated by pollen data (Dräger et al., 2017). Sediment bulk densities were calculated for each sample by dividing the dry weight by the wet sample volume. In addition to the available XRF data (Dräger et al., 2017) bulk phosphorus (P) and titanium (Ti) concentrations were obtained in 4 cm resolution, measured by inductively coupled plasma optical emission spectrometry (ICP-OES; iCAP 7400 Duo, Thermo Fisher Scientific) after acid digestion of the freeze-dried and homogenized sediment material in closed PTFE vessels at 180 °C for 12 h using a HNO_3–HF–$HClO_4$ mixture (Dellwig et al., 2019).

3.2.2. Diatom taxonomy

For diatom analyses the composite profile was subsampled every 1–10 cm in 1 cm thick slices. Diatom sample preparation followed Kalbe and Werner (1974) and Battarbee and Kneen (1982). 0.1 g dry sediment samples were treated with 10 ml of 30% HCL, washed twice with distilled water, followed by centrifugation (12 min, 4000 rpm) and treated with 10 ml H_2SO_4, 1 ml saturated $KMnO_4$ and a few drops of oxalic acid. The samples were rinsed again prior to adding measured quantities of divinyl benzene microspheres (V. Jones, University College London) and embedding diatoms into Naphrax®. Concurrent to counting a minimum of 500 valves, the microspheres were enumerated. Diatom frustule concentrations as number of valves/g DW was calculated using the number of enumerated microspheres according to Battarbee and Kneen (1982). The identification of diatoms was based on (Houk et al, 2010, 2014; Krammer, 1997a, 1997b, 2000, 2002, 2003; Krammer and Lange-Bertalot, 1988; Lange-Bertalot and Moser, 1994; Levkov, 2009).

3.2.3. Biogenic Si (BSi)

The BSi content in TSK sediment samples (n = 141) was determined using a sequential alkaline extraction method (Conley and Schelske, 2001; DeMaster, 1981) and carried out as described in Nantke et al. (2019). Sediment samples are treated with $NaCO_3$ to dissolve the BSi, aliquots withdrawn after 3, 4, and 5 h of reaction, neutralized with HCl and subsequently measured on a SmartChem 200 discrete chemical analyzer as described above. The BSi content was calculated by determining the intercept of a least-squares regression between total extracted Si and extraction time (Conley, 1998; Sauer et al., 2006). Duplicate measurements carried out for 17% of all samples (n = 20) revealed a measurement precision of <6%. Procedural blanks (n = 8) were all below the detection limit.

3.2.4. Si isotope analysis

Sediment sample preparation before isotopic measurements was performed following Morley et al. (2004). In brief, 30% H_2O_2 was used to remove the organic fraction, while heated to 50 °C. Then 5% HCl was added for 2 days to remove carbonates. Heavy liquid separation with sodium polytungstate (SPT) at a density of 2.25 g cm^{-3} was used to separate the mineral fraction from the lighter diatom-bearing fraction, which was subsequently sieved to retrieve the following size fractions: 5–25 μm, 25–53 μm and >53 μm. SPT at a density of 2 g cm^{-3} was used to separate and quantify the clay fraction in the samples 5–25 μm. From the largest fraction (>53 μm) between 400 and 500 diatom frustules and 200–400 sponge spicules were hand-picked under a stereo microscope at 50x magnification. Among the diatom frustules centric (mostly planktonic) and pennate (mostly benthic) diatoms were separated. In samples with low total diatom content in the >53 μm fraction (especially in the upper part of the core) 'mixed' samples were picked (a combination of centric and pennate species) to obtain enough material for the isotope ratio measurements.

The diatom frustules were dissolved in 0.3 ml 0.4 M NaOH at 35 °C for at least 5 days. Cation exchange chromatography following the protocol of Georg et al. (2006) was applied to remove the Na and any other cationic contaminants. All post-column solutions were analyzed by ICP-OES to check for remaining contamination. Samples were diluted to 0.6 (n = 38), 0.5 (n = 20) and 0.4 (n = 8) μg g^{-1} Si in a 0.1 M HCl matrix, doped with a matching Mg concentration and introduced to a Neptune MC-ICP-MS (multi collector inductively coupled plasma mass spectrometer) via an Apex-Q desolvation unit in the HELGES laboratory at the GFZ-Potsdam. Mg isotopes (^{24}Mg, ^{25}Mg, ^{26}Mg) were monitored in dynamic mode to correct for instrumental mass-bias following Cardinal et al. (2003). The Si isotope ratios are expressed in conventional 'delta' notation as a permille (‰) deviation from the same ratio in bracketing analyses of the NBS28 quartz standard. Full analytical protocols are given in Oelze et al. (2016a). Three individual brackets (standard-sample-standard) were averaged for δ^{30}Si and δ^{29}Si. The expected mass-dependent-fractionation gradient of 0.51 in a three-isotope-plot of all 66 samples indicates the absence of polyatomic interferences during mass spectrometry (δ^{30}Si vs. δ^{29}Si, Fig. S1) (Reynolds et al., 2007).

Secondary reference materials were measured throughout the analytical sessions and yielded results in good agreement with expected values: Diatomite (n = 11), with a mean of 1.23 ± 0.08‰ and BHVO-2 (n = 3, mean: 0.26, ±0.07‰) (Reynolds et al., 2007). Typical internal precision of all samples was ca. 0.05‰ and a long-term reproducibility of 0.14‰ (2SD) based on multiple determinations of BHVO-2 over multiple years (Oelze et al., 2016) was used as a conservative estimate of analytical reproducibility.

4. Results

4.1. Water samples

4.1.1. DSi in TSK 2019

The DSi concentrations in the lake water vary between 0.02 and 6.2 mg SiO_2 L^{-1}, depending on season and water depth (Fig. 2A). During January and February DSi is uniformly distributed throughout the water column with values between 3.0–3.5 mg SiO_2 L^{-1}. In March the surface water DSi concentrations (0–25 m) begin to decline until DSi becomes almost totally depleted in the uppermost 3 m by the end of May. In June DSi concentrations in the bottom waters (35–50 m water depth) start to increase, until maximum values of around 6 mg SiO_2 L^{-1} are reached at the end of October (Fig. 2A). In December the stratification breaks down again, distributing the DSi homogenously and producing concentrations of ~3 mg SiO_2 L^{-1} throughout the water column (Roeser et al., 2021).

4.2. Sediment samples

4.2.1. Diatom taxonomy

The diatom taxonomy shows the dominance of planktonic, bloom forming diatom species from the genera *Cyclotella, Stephanodiscus* and *Aulacoseira* in Tiefer See. The c/p (centric/pennate) ratio however has a minimum around 250 a BP indicating more benthic (pennate) diatom species in the lake (Fig. 4). The dominant

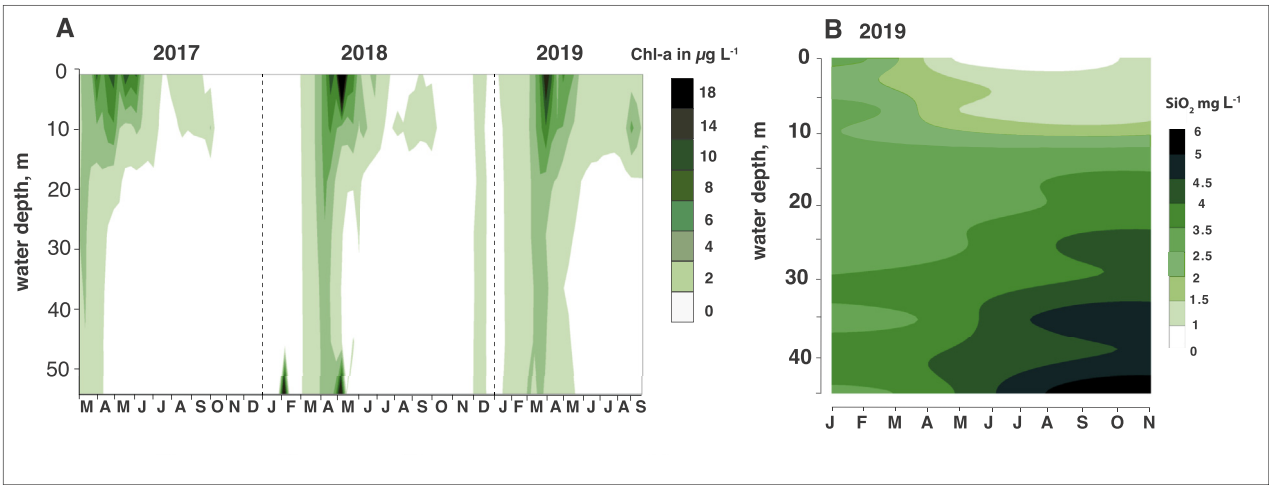

Fig. 2. **A** Chlorophyll-a concentration (µg L^{-1}) in the TSK water column measured with a multiparameter profiler in 2 m intervals between 1 and 53 m water depths measured within the monitoring of Tiefer See since May 2012 (Roeser et al., 2021). Displayed are the results for March 2017 until September 2019. **B** Contour-plot of the DSi (SiO_{2L} $_{L^{-1}}$) concentrations in the water column of TSK during 2019. The underlying DSi profiles were measured using molybdate-blue methodology at six different water depths (Eggimann et al., 1980). (For interpretation of the references to colour in this figure legend, the reader is referred to the Web version of this article.)

benthic species belong to the genus *Staurosira*. A complete taxonomical study on the diatoms from Tiefer See will be published elsewhere.

4.2.2. Biogenic Si (BSi)

The contents of BSi in TSK sediments vary between 1 and 38% SiO_2 within the investigated upper 600 cm TSK sediments covering the last ~4300 years (Fig. 3). In the lower part of the record (600–570 cm depth, 4230–4000 a BP) BSi contents are moderate (between 5 and 10%) and then decrease to values between 1 and 2%, with a minimum of 0.97%, around 550 cm depth (3680 a BP). An increasing amount of BSi between 510 and 360 cm sediment depths (3170–1870 a BP) varies between 2.5 and 9.8%. Between 360 and 110 cm (1870–370 a BP), the BSi content is generally high (above 10%) with the exception of a few isolated samples, and reaches a maximum of 38% at 240 cm, 1070 a BP. Between 110 and 80 cm

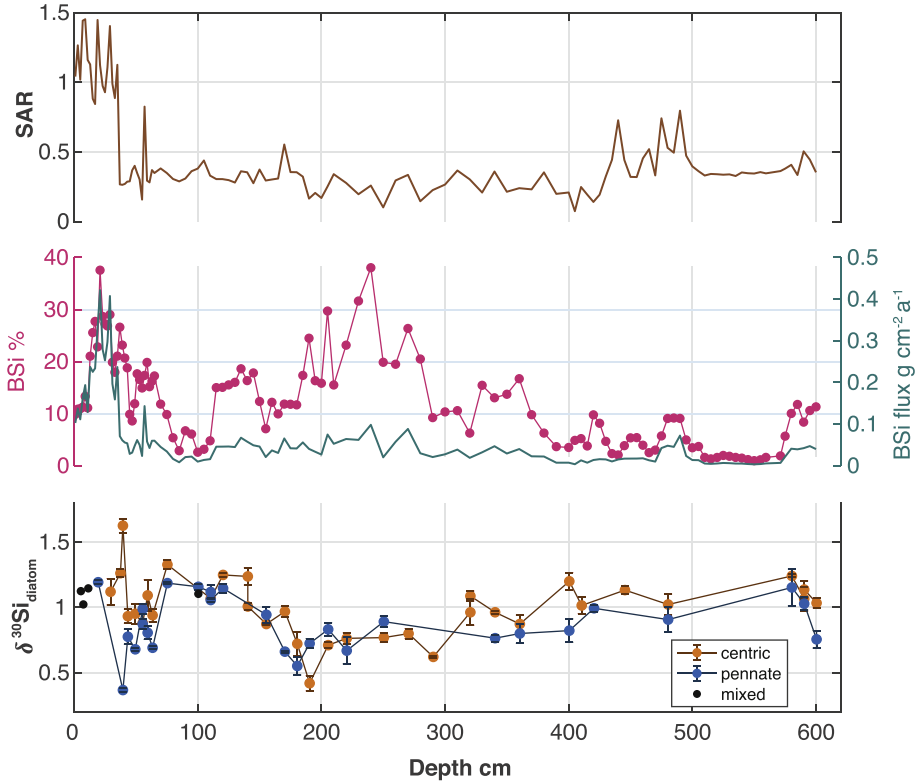

Fig. 3. Sediment accumulation rate (SAR), measured biogenic silica (BSi) in %, calculated BSi flux and $\delta^{30}Si_{diatom}$ (pennate = blue dots, centric = orange dots and mixed samples = black dots) in TSK sediments in the uppermost 600 cm of the sediment composite profile. (For interpretation of the references to colour in this figure legend, the reader is referred to the Web version of this article.)

sediment depth (370–200 a BP) BSi contents are lower (3.5–6.6%) but increase again to values between 8.6 and 37.5% throughout the topmost 75 cm (last ~270 years). BSi fluxes are calculated using sediment accumulation rates (SAR = sedimentation rate*bulk density) (Fig. 3). The resulting BSi fluxes range from 0.003 to 0.421 g SiO_2 m^2 a^{-1}. Since the SAR is relatively stable through nearly the entire period, BSi contents and BSi fluxes resemble each other. However, increasing sedimentation rates in the top 35 cm of the core (last ~90 years), driven by calcite precipitation within the lake, lead to a ca. 5x increase in SAR and consequently in BSi flux within only 40 years (47–7 a BP, 1903–1943 CE). Because the BSi flux data is dominated by this large increase, masking the changes in the older part of the record, we focus on BSi contents in the discussion.

4.2.3. δ^{30}Si isotopes in diatom frustules

The Si isotope composition of the hand-picked diatoms varies between 0.37 and 1.63‰, with a mean of 0.95‰ (Fig. 3). Both centric and pennate diatom data-series, ($\delta^{30}Si_{centr}$ and $\delta^{30}Si_{penn}$, respectively) show similar trends during the last 4230 years. Values vary between 0.76 and 1.24‰ at the beginning of the record from 600 to 580 cm sediment depth (4230–4040 a BP). A lack of sufficient diatom frustules in the >53 μm fraction between 580 and 480 cm depth (4040–3000 a BP, see BSi section above) precluded determination of diatom δ^{30}Si here, but from 480 to 190 cm sediment depth (750–300 a BP) the data show a gradual decline to a minimum $\delta^{30}Si_{centr}$ value of 0.42‰. From 190 to 75 cm (300–200 a BP) the isotope values increase again to a $\delta^{30}Si_{centr}$ maximum of 1.33‰. Simultaneously a decline with a minimum of 0.37‰ for $\delta^{30}Si_{penn}$ (39 cm, 36 a BP) is followed by a steep increase at 37 cm sediment depth (26 a BP) to 1.19‰ in $\delta^{30}Si_{penn}$. The topmost 35 cm (last 90 years) of the TSK sediment core show Si isotope compositions of 1.02–1.26‰; note that these data comprise centric and pennate diatoms (see methods).

4.2.4. Phosphorus (P) and titanium (Ti) in the sediment core

Phosphorus (P) contents vary between 0.06 and 3.42 wt%, and titanium (Ti) fluctuates between 0.005 and 0.36 wt% within the investigated period. Their pathways through time are anti-correlated: if Ti is high, P is low and vice versa. We calculated fluxes for both elements to correct for changes in sediment accumulation rates as described for BSi (element content (%) * SAR). As with BSi, the calculated fluxes describe the same trends as the element content (Fig. 4).

5. Discussion

Previously published paleolimnological data from multiple sites demonstrate considerable human activity since around 4000 a BP in northeastern Germany (Kappler et al., 2018; Selig et al., 2007; Wieckowska et al., 2012). At TSK deforestation and the establishment of agriculture have been shown to impact both the terrestrial ecosystem and the lake development (Dräger et al., 2017). Previous work on TSK sediments has demonstrated (via XRF Si/Ti ratios), a >10 fold variability in BSi concentration for the last 4300 years (Dräger et al., 2017), corroborated here with our alkali leaches. The diatom composition of the last 2000 years show variations in centric/pennate "c/p" ratio together with BSi concentrations, indicating changes in habitat and nutrient conditions (Fig. 4) (Cooper, 1995). In combination, these studies suggest that the Si cycle in TSK and its catchment has changed in response to human activity. Limnological monitoring at the lake since 2012 including pH, O_2 and Chlorophyll-a measurements, can help to improve our understanding of the modern lake system (Dräger et al., 2017; Roeser et al., 2021; Theuerkauf et al., 2015) and Si cycling in particular.

5.1. Modern phytoplankton abundance and DSi availability

To guide our paleo-interpretations, we use Chlorophyll-a (Chl-a) and DSi concentrations measured in the water column of TSK (Fig. 2A and B) to constrain modern Si cycling in the lake ecosystem. The concentrations of Chl-a show a large spring bloom and a second but less pronounced peak in productivity in autumn. Decreasing DSi concentrations in the uppermost water layers during April reflect the dominance of diatoms during this period, which depletes DSi until late summer/autumn (Fig. 2B).

Annual differences in the timing and length of the spring diatom bloom, and the phytoplankton population size are linked to changes in water column mixing (length and timing), winter temperatures (ice cover), nutrient input and recycling rates. During winter, homogeneous temperatures of 4–5 °C, imply a well-mixed water body explaining uniform DSi concentrations in the water column. The onset of lake stratification in late March/April combined with diatom production and DSi uptake in the surface photic layer during the spring bloom leads to essentially complete DSi depletion down to 0.2 mg SiO_2 L^{-1} in the surface water in 2019 (Fig. 2B) (Dräger et al., 2017; Kienel et al., 2013).

By contrast, the bottom waters remain more enriched in Si throughout the year. Bottom-water DSi maxima in summer and autumn of 5–6 mg L^{-1} most likely reflect a combination of sinking diatom dissolution, pore water DSi diffusion back into the water column following diatom dissolution in the sediment, and DSi inputs via groundwater. Diffusion of DSi across the sediment-water interface is a potentially important mechanism of recycling for dissolved elements, including DSi, as demonstrated for marine ecosystems (Frings, 2017; Geilert et al., 2020). As the stratification breaks down in autumn/early winter, and with only minor amounts of winter biosiliceous production, DSi becomes again distributed throughout the water column until the beginning of the following spring bloom (Fig. 2B).

In TSK we estimate a Si residence time τ_{res} (defined as $\tau_{res} = M_{Si}/F_{in}$, where M_{Si} is the inventory of Si in the lake water and F_{in} is the total annual input of DSi) of about 3 years. Briefly, we calculate the inventory based on the average DSi concentration measured through the water column in 2019 (3.1 mg L^{-1} SiO_2) and the volume of the lake (~13.5 km^3), to yield an inventory of 41.9 t SiO_2. Since the modern lake has no continuous in- and outlet, fluxes of DSi from the watershed are hard to monitor or estimate and we therefore take an average DSi yield from a variety of North American catchments of 2.68 t SiO_2 km^{-2} a^{-1} (Jansen et al., 2010) as a first-order approximation. Combined with the watershed area of TSK (5.5 km^2), this yields annual inputs of 14.7 t SiO_2 a^{-1}. In the end, a residence time of 2.8 years (i.e. 41.9 t/14.7 t a^{-1}) can be estimated. While only an order-of-magnitude approximation, this implies that after about 3 years the Si inventory of the lake is replaced, and changes in Si isotope ratios over longer timescales are more likely driven by inputs than e.g. internal redistribution. Recycling of diatoms in the water column, or other processes internal to the lake, only play a role for short term (<3 years) changes. This residence time serves as an approximation and may be an overestimate, since it is not known to what degree possible sources like groundwater, are integrated in the estimate of Jansen et al. (2010). For our study we consider 3 years as the maximum Si residence time in TSK.

5.2. Mid to late holocene evolution of BSi burial in TSK sediments

Biogenic silica accumulation rates and diatom community compositions are well-established tools to reconstruct aspects of past lake productivity and provide the basis for δ^{30}Si data interpretations. In TSK, Dräger et al. (2017) identified two important

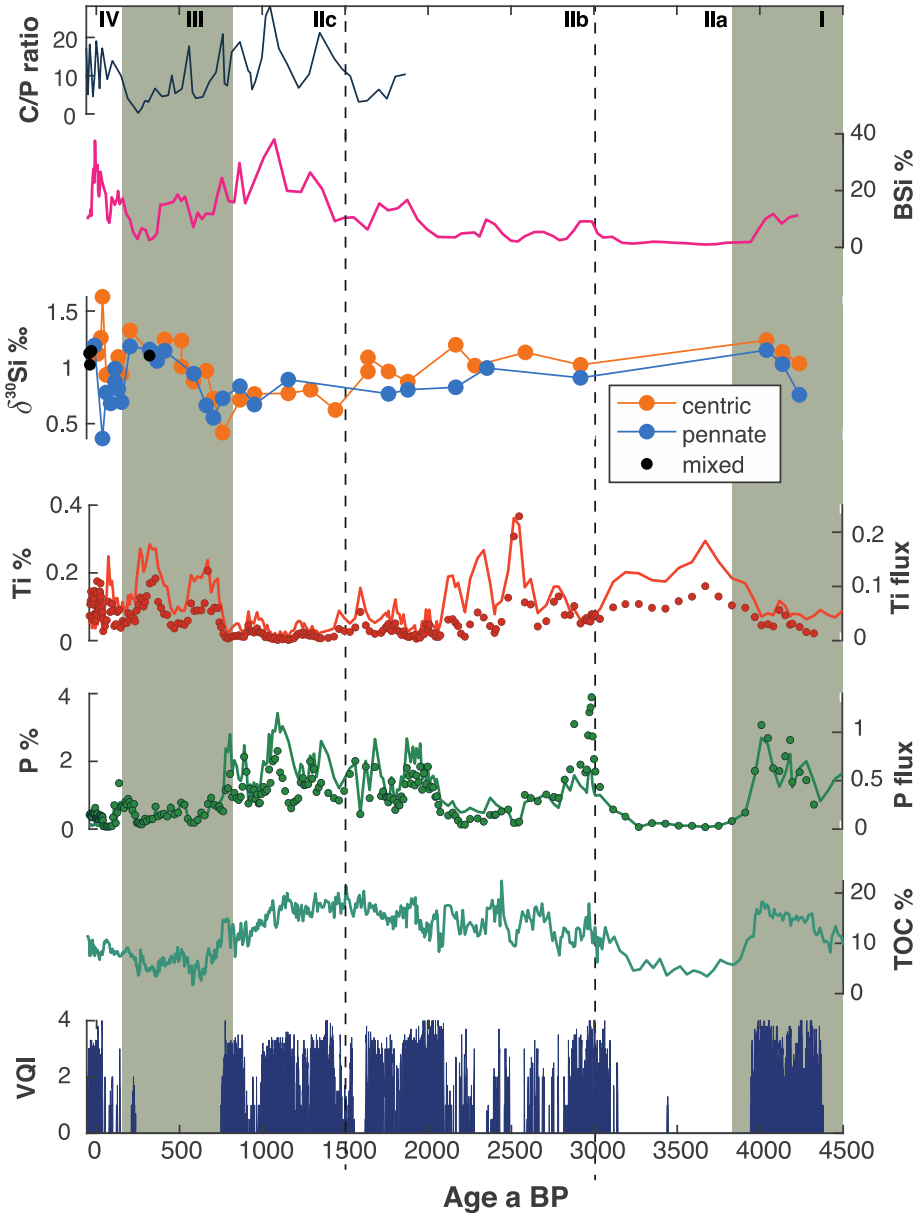

Fig. 4. c/p (centric/pennate) ratio, BSi (%), δ^{30}Si (centric diatoms (orange dots), pennate diatoms (blue dots), mixed diatoms (black dots), titanium in % and calculated flux in g cm^{-2} a^{-1} (red dots), phosphorous in % and calculated flux in g cm^{-2} a^{-1} (green dots), total organic carbon (%, TOC) and varve quality index (VQI) plotted for the last 4300 years (Dräger et al., 2017). Units I-IV are highlighted by alternating grey and white shaded areas. Higher VQI values reflect improved varve preservation. (For interpretation of the references to colour in this figure legend, the reader is referred to the Web version of this article.)

influences on the strength and intensity of water column overturning and varve preservation within the last 6000 years: 1) climate (especially wind stress), and 2) vegetation openness, due to human activity. Phases with more frequent and/or intense water column overturning cause oxygenation of the bottom water that impedes varve formation. These phases alternate with periods characterized by longer and/or stronger stratification, conditions that promote the preservation of varves, due to anoxic bottom waters. These changes are encapsulated in the 'varve quality index' (VQI), describing the preservation of varves in the sediment core (Fig. 4, from Dräger et al., 2017). The frequency of lake overturning is also a key influence on physical and chemical conditions in a lake, including the availability and distribution of nutrients, oxygen, pH, light conditions and temperature. These parameters directly or indirectly influence diatom growth, species composition and BSi dissolution (Loucaides et al., 2008; Williams and Crerar, 1985). Correspondingly, the changing BSi contents and composition in TSK sediments over the last 4300 years can be linked to environmental conditions and corroborate previous paleolimnological interpretations.

In the beginning of the record (4300–4000 a BP) both diatoms and siliceous sponges are present in the sediments at sizes up to 80 μm, identified with light microscopy and SEM. Most likely spicules are redistributed from shallower, oxygenated parts of the lake, likewise resuspended sediment becomes integrated in the varved sections (Roeser et al., 2021). The available data suggests a forested catchment (e.g. high tree pollen counts, Fig. 5) and low detrital input (indicated by low Ti fluxes, Fig. 4).

A windier period between 4000 and 3100 a BP with an increased vegetation openness (Dräger et al., 2017), favored turbulent water

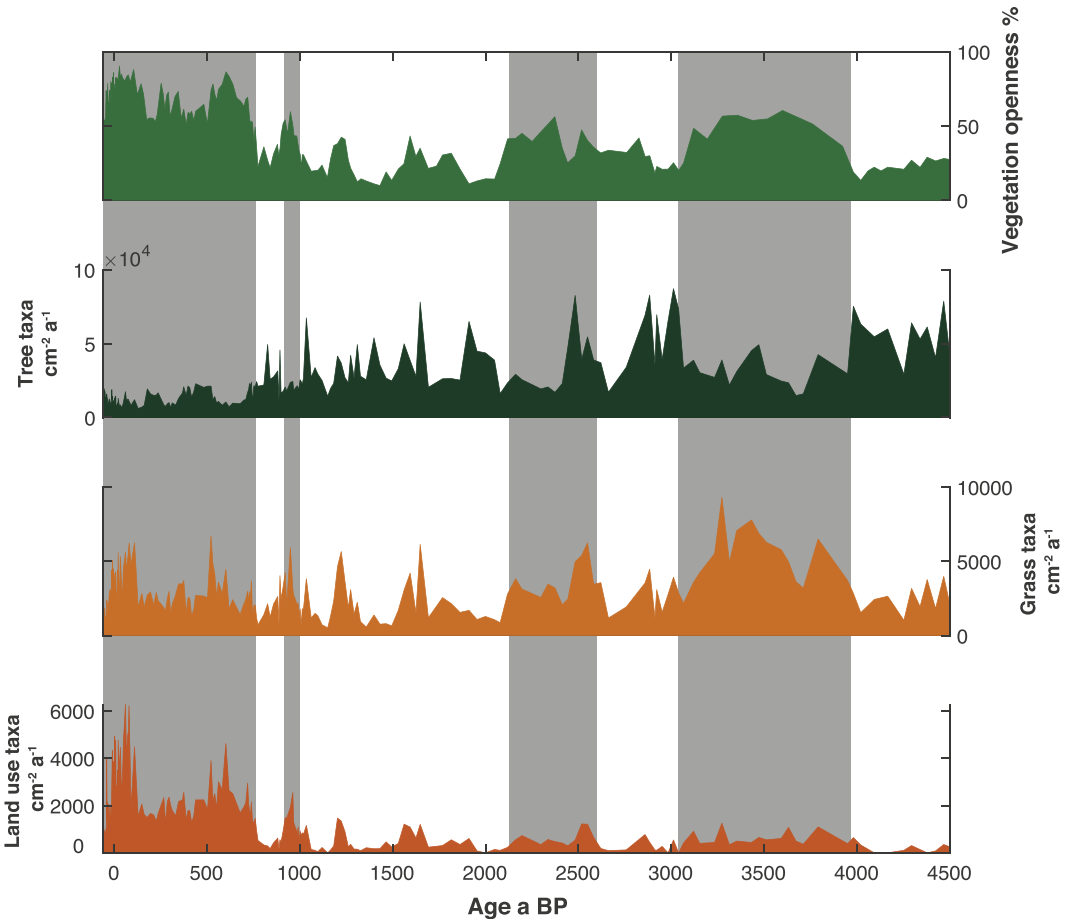

Fig. 5. Pollen counts from the Tiefer See composite profile since 4500 a BP: the sum of tree taxa pollen forest cover, the sum of grass taxa pollen indicating land openness independent from agriculture and land use pollen (comprising *Rumex*, *Secale* and *Cerealia*) showing land cultivation in the catchment. Vegetation openness was calculated from pollen percentage data using the REVEALS model. Grey shaded areas indicate settlement phases in the TSK catchment after Dräger et al. (2017).

column conditions and the transport of suspended detrital material (indicated by bulk Ti concentrations and Ti fluxes). An increased frequency and/or intensity of lake overturning enhanced the redistribution of oxygen and nutrients in the lake, favored the growth of benthic sponges and the accumulation of their spicules. In contrast, diatom frustules in the sediment are rare and mostly <20 μm, implying adverse growth conditions that lead to an increase in vegetative proliferation of cells, most likely caused by decreasing light availability and perhaps even by increased competition for DSi with sponges. Additionally, oxygenated bottom waters favor aerobic decomposition at the sediment water interface and thus decrease BSi preservation (Bidle et al., 2003). Relatively small diatoms likely favored BSi re-dissolution in the water column and in the sediments after deposition. At the same time, increases in *Rumex* and decreases in tree pollen suggest a more open landscape caused by intensified human land use in the lake catchment since ~3900 a BP leading to a reconstructed vegetation openness exceeding 50% (Dräger et al., 2017) (Fig. 5).

The reappearance of well-preserved varves around 3000 a BP, which largely persist until about 750 a BP, reflects a shift back to a predominantly stratified lake with anoxic bottom waters, a loss of benthic habitats and a diatom-dominated ecosystem. Increasing BSi contents around 1500 a BP likely reflects additional DSi inputs from catchment soils into the lake that further favor the dominance of diatoms within the phytoplankton community in TSK (Fig. 4). At around 750 a BP, the varve quality abruptly drops to zero, implying largely oxic bottom waters and more frequent overturning. Elevated Ti fluxes at the same time imply slightly increased detrital inputs during the Little Ice Age in Europe (550–250 a BP) (Fig. 4) (Mann et al., 2009). Pollen counts imply an increasingly deforested catchment, and BSi contents and accumulation rates decrease (Fig. 5). Together, the implication is that windier conditions induce water mixing and sediment resuspension, and thus increase water column turbidity that in turn limits diatom production. The last 150 years are more challenging to characterize. The return of varved sediments, abrupt variations in BSi contents and very small mostly planktonic diatom frustules i.e. dominated by *Aulacoseira subarctica*, *Stephanodiscus medius* (Kienel et al., 2013) and *Stephanodiscus parvus*, suggest an eutrophic environment with elevated fluxes of nutrients, as observed in other northern European lakes (Bradshaw et al., 2005).

5.3. $\delta^{30}Si_{diatom}$ as a proxy for changing Si inputs

Previous studies have highlighted how changes in Si isotope composition can provide additional insight into climate or human impacts on the alteration of the Si cycle in freshwater ecosystems (e.g. Nantke et al., 2019a; Swann et al., 2010). Working on an East African crater lake, Street-Perrott et al. (2008) were the first to attempt to link diatom $\delta^{30}Si$ to catchment Si cycling. Subsequently, large-scale changes in land use, especially extensive deforestation for agricultural use, have been shown to increase $\delta^{30}Si$ of soil waters and adjacent aquatic ecosystems through the preferential export of ^{28}Si from soil pools, via erosion and crop harvest (Nantke et al.,

2019; Vandevenne et al., 2015). Elsewhere, diatom $\delta^{30}Si$ data from the Siberian lakes El'gygytgyn and Baikal indicate the importance of large-scale temperature changes and nutrient recycling for controlling $\delta^{30}Si_{diatom}$ values in oligotrophic lakes in the absence of human activity (Swann et al, 2010, 2020). In Lake Edward and Lake Victoria (East Africa), Cockerton et al. (2015) inferred a climatic control on the $\delta^{30}Si$ of DSi delivered to the lakes over the last deglacial cycle. Increasing temperatures and humidity favor chemical weathering and increased DSi fluxes from river catchments. Consequently, enhanced DSi concentrations in the lakes cause a shift towards lower $\delta^{30}Si_{diatom}$. For TSK, different lines of evidence suggest the importance of the $\delta^{30}Si$ of DSi supplied to the lake in determining the $\delta^{30}Si_{diatom}$ record.

Our data show that high BSi burial fluxes are associated with high nutrient conditions and anoxic bottom waters, as indicated by both elevated P contents and enhanced varve preservation 1600–750 a BP and since 150 a BP, Fig. 4. However, a lack of correlation between $\delta^{30}Si_{diatom}$ and BSi contents ($r^2 = 0.13$, $p = 0.31$) (Fig. 6) in TSK sediments, indicates the dominance of the $\delta^{30}Si_{DSi}$ in setting $\delta^{30}Si_{diatom}$. If utilization was the important control, we would expect a correlation between productivity (proxied by BSi MAR) and diatom $\delta^{30}Si$. The short-inferred residence time for DSi in the lake (see above), relative to the timescale of our $\delta^{30}Si$ record, also implies that transient effects or recycling of BSi are unlikely to affect $\delta^{30}Si$ over decadal or longer timescales.

Further, the similar trends between $\delta^{30}Si_{centr}$ and $\delta^{30}Si_{penn}$ for most of our record, independent from changing lake conditions through time (indicated by VQI, OM and BSi; see above) also suggest the $\delta^{30}Si$ of the DSi inputs to be the predominant influence on $\delta^{30}Si_{diatom}$. Since the centric diatoms that we hand-picked are bloom-forming species living in the surface water column and the pennate taxa are more frequently benthic and non-bloom forming, the similarity between both isotope signals could tell us about the source of DSi. The long-term agreement between both isotope signals, despite changing circulation pattern and preservation of organic matter (Fig. 4), suggests that the $\delta^{30}Si_{DSi}$ is more influenced by inputs than by internal cycling in the lake. If this were not the case, we would expect to see larger deviations between the trends of both records ($\delta^{30}Si_{centr}$ and $\delta^{30}Si_{penn}$) over time: making the assumption that the pennate and centric diatoms grow in different periods of the year and live in different parts of the water column, changes in internal nutrient recycling would impact the Si isotopes of both groups in unequal ways. Slight divergences between the two signals (Fig. 3) could be caused by smaller shifts in the growing season, species composition (i.e. species-specific fractionation) or onset of stratification.

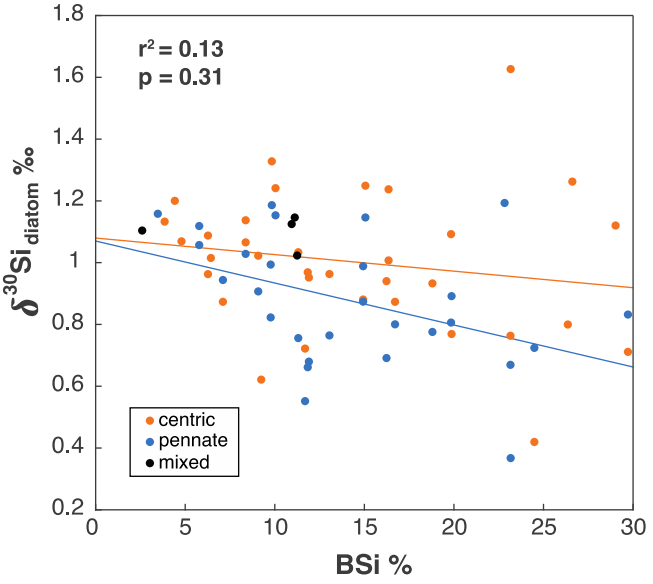

Fig. 6. BSi content (%) plotted against $\delta^{30}Si_{diatom}$ for the last ~4300 years in Tiefer See. Centric diatoms (orange dots), pennate diatoms (blue dots) and mixed diatom samples (black dots). The regression lines are shown for centric diatom values (orange line) and pennate diatom values (blue line). (For interpretation of the references to colour in this figure legend, the reader is referred to the Web version of this article.)

In the modern lake DSi is depleted during the spring diatom bloom, which makes $\delta^{30}Si_{diatom}$ in the sediment dependent upon the $\delta^{30}Si$ of DSi supplied to the photic zone. As described in the introduction, and in Nantke et al. (2019), $\delta^{30}Si_{diatom}$ values are determined by two key parameters: the $\delta^{30}Si$ of DSi during the growth period ($\delta^{30}Si_{DSi}$, Si source) and the relative DSi utilization controlled by diatom production (as recorded by the BSi burial flux, e.g. the Si sink). The formation of diatom frustules is associated with a Si isotope fractionation around −1‰, which means that the residual DSi becomes enriched in ^{30}Si (higher $\delta^{30}Si$) (De la Rocha et al., 1997). However, when all available DSi is converted to diatom BSi, then $\delta^{30}Si_{diatom}$ must equal the source $\delta^{30}Si_{DSi}$, since the isotope difference between initial $\delta^{30}Si_{DSi}$ and $\delta^{30}Si_{diatom}$ is zero at complete conversion of DSi to BSi. The available data from sediment trap studies (Closset et al., 2015; Panizzo et al., 2015) suggests that the fraction of diatom BSi that survives dissolution preserves the initial signal, with no associated fractionation. Assuming a near-complete DSi utilization (Fig. 2B) throughout the late Holocene (at least the last 4000 years), the $\delta^{30}Si_{diatom}$ in TSK provides a faithful record of the $\delta^{30}Si_{DSi}$ supplied to the diatoms through the growing season. However, this assumption is not necessarily valid for the whole record, for example between 3900 and 3000 a BP (Fig. 4) low BSi fluxes might have led to higher DSi concentrations in the water column of TSK, if the spring and autumn blooms were not sufficiently large to deplete the water of DSi.

The silicon isotope record from TSK sediments can be divided into four main units reflecting the (I) initial situation before major human activity (4300–3900 a BP), (II) a period of early deforestation (3900–750 a BP), (III) intensified cultivation period (750–150 a BP) and (IV) the modern eutrophic period (last 150 years)(Fig. 4).

5.3.1. Unit I: 'Initial setting before major human activity' 4300–3900 a BP

Unit I represents the initial situation before the onset of major human activity in the TSK catchment. Pollen data point to a largely forested landscape with an 'openness' of ~30% (Fig. 5). The lake level was 2–3 m lower than today, suggesting the isolation of TSK from its neighboring lakes Flacher See to the North and Hofsee to the South (Fig. 1). With only a few $\delta^{30}Si_{diatom}$ data points, it is hard to conclusively characterize the Si cycle, but relatively high isotope ratios (average of 1.06‰) provide a baseline with which to compare the later, human impacted system. Using the conceptual model from Struyf et al. (2010) the catchment Si cycle was likely dominated by intensive Si cycling at the vegetation-soil interface and characterized by a large inventory of amorphous Si in the soil. In a pre-human ecosystem at steady-state, with a constant Si inventory, the isotopic composition of Si exported from soils must equal the Si entering the system. With weathering of silicate minerals as the only significant Si input into the soil-plant system, the measured $\delta^{30}Si_{diatom}$ value of ~1‰ must reflect the $\delta^{30}Si$ of DSi released during the net weathering process. A large Si soil pool buffers small-scale changes in the terrestrial loop (see introduction) (Cornelis and Delvaux, 2016; Vandevenne et al., 2012).

Individual benthic diatom frustules are maximum 80 μm in their longest dimension, however the population is dominated by smaller planktonic species. Sponge spicules found in this period

were probably laterally transported from more shallow lake areas (see above). This relatively undisturbed period of the lake system before intensified anthropogenic land use serves as the initial situation to discuss changes in Si cycling linked to human activity.

5.3.2. Unit II: 'Early deforestation period' 3900–750 a BP

Unit II is generally characterized by deforestation in favor of cultivation and a declining trend in $\delta^{30}Si_{diatom}$ of around 0.7‰ over ~3000 years. Based on shifts in water overturning and detrital input (Fig. 4), we divide this unit into sub-units IIa (3900–3000 a BP), IIb (3000–1600 a BP) and IIc (1600–750 a BP).

In sub-unit IIa the BSi contents decrease abruptly to ~1%, implying low diatom production and/or low frustule preservation in the sediment. The few preserved diatoms are small (<25 μm). Enhanced water overturning, indicated by the absence of varves (Kienel et al., 2013) favor oxygenated bottom waters and the presence of siliceous sponges in sub-unit IIa (Fig. 4). A decreasing trend in $\delta^{30}Si_{diatom}$ between 3000 until 750 a BP (sub-units IIb and IIc) is recorded in both $\delta^{30}Si_{centr}$ and $\delta^{30}Si_{penn}$ and coincides with intensified land use and deforestation, supported by the increase in pollen counts associated with land use (Figs. 4 and 5) (Dräger et al., 2017). During the early deforestation period (~3900–1500 a BP), as evidenced by decreasing tree taxa pollen (Fig. 5), we interpret an enhancement of DSi export rates from the catchment as the dominant process influencing the Si cycle in TSK. The uptake of preferentially light ^{28}Si of crops and grasses and the removal via harvesting seems to be negligible here, since the size of the soil pool in this period is still rich in light Si isotopes and the cultivation might not be intense enough to deplete it (Cornelis et al., 2014).

Part of the explanation for the long-term decrease in $\delta^{30}Si_{diatom}$, lies in the transient depletion of the low$\delta^{30}Si$ soil ASi pool. As suggested by Struyf et al. (2010) it is likely that DSi export rates from the soil ASi pool were enhanced, releasing ^{28}Si-enriched DSi to the soil water, and ultimately the lake. Expected low $\delta^{30}Si_{DSi}$ in the soils of the catchment thus led to a decreased $\delta^{30}Si_{DSi}$ in the water column of TSK and consequently $\delta^{30}Si_{diatom}$. Based on the findings by Clymans et al. (2011), Vandevenne et al. (2015) and Nantke et al. (2019a) we would expect to see a transient enhancement in Si export following deforestation as the soil ASi pool depletes to persist on decadal timescales, followed by a stabilization, when it reaches a new, lower, steady-state. The long-term trend, with continuously decreasing $\delta^{30}Si_{diatom}$ through Unit II (>2000 years), therefore suggests other processes involved. Secondary clay minerals are also associated with low $\delta^{30}Si$ (Frings et al., 2016) and may dissolve and contribute to the DSi soil pool available for plant uptake (Cornelis and Delvaux, 2016). Having a longer reactivity time than ASi (phytholiths), their importance as the main Si source might increase as the ASi soil pool gets depleted. In a controlled soil-plant-solution experiment Li et al. (2020) have shown that clays and ASi both contribute to the vegetation feedback loop: with dissolving clays being the ultimate source for Si while ASi dissolution is the proximate control on plant Si uptake. To investigate this source of Si in the catchment of TSK, the measurement of Ge/Si ratios or $\delta^{30}Si$ in clay minerals would be needed. We surmise that a change in Si (re)cycling at the vegetation-soil interface, as forested ecosystems are replaced with croplands and meadows, would alter weathering reactions and the export fluxes of DSi, clay minerals and BSi.

There are several mechanisms that could alter Si isotope partitioning as a function of ecosystem structure. For example, below ground pCO_2, organic acid concentrations, soil-solution chemistry, and the presence and abundance of mycorrhiza fungal networks are all related to the aboveground biomass. They also all affect the rate at which primary silicate minerals are attacked, and secondary minerals precipitate. Since the ratio of secondary mineral formation to primary mineral dissolution is the key control on silicon isotope distributions in the Critical Zone (Bouchez et al., 2013; Frings et al., 2016), it is expected that Si isotope partitioning will change as the ecosystem is altered. The precise combination of processes is hard to define, but the net result likely includes a change in clay-mineralogy. We arrive at this conclusion by observing that the same mass-balance constraints that apply to diatom silica production (see above) also apply to secondary clay mineral precipitation (Opfergelt et al., 2012). A decrease in DSi $\delta^{30}Si$, as we interpret from our diatom records, therefore means that progressively more Si is partitioned towards DSi at the expense of Si in clays. This means that weathering beneath cropland and meadows produces more Si-poor clays than forests. Altogether this could explain the decrease in $\delta^{30}Si$. While detailed studies are necessary to better understand and disentangle these processes, the data presented here is strong empirical evidence for a change in net weathering-reaction stoichiometry – and therefore $\delta^{30}Si$ of DSi – in response to changing ecosystem structure (Tye et al., 2009). To further investigate the sources of Si in the catchment of TSK, future work could seek to exploit geochemical proxies sensitive to clay mineral formation, e.g. lithium or magnesium isotope ratios.

A further intensification of agriculture in sub-unit IIc (1600–750 a BP) – as indicated by elevated P fluxes (Fig. 4) – occurs synchronously with an increase in c/p ratio and BSi flux to a maximum of ~0.1 g cm^{-2} a^{-1} (38% BSi) 1073 a BP). The dominance of the diatom species *Cyclotella comensis* in this sub-unit between ~2000 and 700 a BP might point to longer ice cover in spring favoring short, but deep-water column mixing and enhanced nutrient recycling. Specific diatom species, e.g. *Cyclotella comensis* benefit from these conditions in TSK, due to their competitive advantage of growing under the ice (Kienel et al., 2017).

5.3.3. Unit III: 'Intensified cultivation period' 750–150 a BP

In Unit III an increase in $\delta^{30}Si_{diatom}$ is probably driven by an increase in land cultivation and the associated harvest of crops, which preferentially take up ^{28}Si. Due to the enhanced export of light ^{28}DSi in unit II we here assume an already depleted Si soil pool.

Low varve preservation implies shorter seasons of stratification and prolonged periods of oxygenated bottom waters in TSK between ~750 and ~150 a BP (VQI, Fig. 4). The climate deterioration observed in Europe during the Little Ice Age (550–250 a BP) was manifest in northern Germany as cooler, wetter and windier conditions (Mann et al., 2009). Consequently, water circulation improved nutrient and oxygen distribution in the lake favoring benthic living organisms as suggested by the low c/p ratio (Fig. 4). At the same time, increasing abundances of *Secale* und *Cerealia* pollen document an intensification in crop cultivation in the catchment of TSK (Fig. 5). Simultaneously, increasing $\delta^{30}Si$ values (by ~0.8‰ over 500 years) indicate a shift to a heavier Si source compared to the early deforestation period between 3000 and 750 a BP (Units IIb and c). In Unit III, the BSi content is relatively low (average of 10% and Si flux of 0.04 g cm^{-2} a^{-1}) and probably not the main control on the $\delta^{30}Si_{diatom}$ signal (Fig. 4): low DSi utilization would result in lower diatom $\delta^{30}Si$, considering all other Si inputs and outputs to be stable.

The most likely explanation for an increasing $\delta^{30}Si_{diatom}$ is a heavier isotope pool in the watershed. The growth and harvest of an increasing number of crops in the catchment, which also discriminate against the heavier isotopes of Si during uptake, would lead to a preferential removal of the lighter ^{28}Si isotopes from the catchment (Frick et al., 2020; Vandevenne et al., 2015). The high DSi demand of many crop species (Cooke et al., 2016) enhances the Si removal from the soil pool. Low Si export rates from depleted soils with a ^{30}Si enriched isotope composition then

determines the local terrestrial Si cycle in the watershed and potentially the adjacent lake (Struyf et al., 2010). The relatively small catchment of TSK allowed small-scale agriculture, but an open question is the degree to which harvested crops were exported from the area (and thus the catchment Si pool). Only few settlements directly adjacent to the lake would support the interpretation that the harvested Si was consumed elsewhere, and thus not returned (via humans) to the lake system (Dräger et al., 2017; Selig et al., 2007). This crop-Si therefore became largely unavailable for the diatom production in the lake. Thus, we infer that the ca. 0.8‰ increase in diatom $\delta^{30}Si$ in Unit III reflects crop harvesting, associated with a preferential removal of the lighter ^{28}Si.

5.3.4. Unit IV: Modern eutrophication since ~150 a BP

The modern Si isotope signal since around 150 a BP is most likely influenced by the interplay between agriculture (including intensified fertilizer application) and increased diatom production. Increasing air and water temperatures since the Little Ice Age favored productivity and summer stratification, leading to anoxic bottom waters and the reappearance of varves in the sediment record.

Within the last century the vegetation in the catchment of TSK changed as a result of more intensive landscape cultivation than in the rest of the human-inhabited period (Theuerkauf et al., 2015). This is reflected in a further steep increase in *Cerealia* pollen, which co-occurs with the dominance of centric (planktonic) diatom taxa, especially *Stephanodiscus parvus*, that are associated with eutrophication. Abruptly increasing SAR since around 1930 CE is driven by calcite precipitation (Dräger et al., 2017), triggered by increases in pH that follow peaks in primary production. Sediment BSi contents vary between 10 and 37% (equivalent of fluxes of 0.01–0.42 g cm^{-2} a^{-1}) indicating rapid changes in Si input, Si source and/or DSi utilization. Elsewhere, it is well established that BSi fluxes are sensitive indicators of eutrophication (e.g. Heathcote et al., 2014): given sufficient DSi, diatoms often tend to outcompete other phytoplankton groups in competition for P. Schelske et al. (1983) showed how ongoing eutrophication in the North American Great Lakes led to diatom production depleting the water DSi inventory, and thus switching the diatoms from P-limited to Si-limited. This was manifest in the sediment record as a transient increase followed by a new, lower, steady-state BSi accumulation rate. After the DSi reserve in the lake is depleted the Si cycle is more sensitive to inputs from the watershed, i.e. it lacks the buffering capacity that covers small scale changes in DSi supply.

$\delta^{30}Si_{centr}$ and $\delta^{30}Si_{penn}$ both vary around 1‰, except in the 1920s when the records deviate from each other for the only time in the last 4300 years, with lower $\delta^{30}Si_{penn}$ and higher $\delta^{30}Si_{centr}$ (min: 0.37‰, ~36 a BP, $\delta^{30}Si_{penn}$; max: 1.63‰, ~36 a BP, $\delta^{30}Si_{centr}$)(Fig. 7). This difference might be caused by long winter ice covers and a maintained stratified water column during the main diatom bloom of the following year. Alternatively, enhanced dissolution of BSi in the uppermost sediments and diffusion of DSi across the sediment-water interface might impact benthic diatom $\delta^{30}Si$, especially when water column stratification is stronger.

Relatively stable $\delta^{30}Si_{diatom}$ since the 1920s with values between 1.02 and 1.15‰ were measured on mixed diatom samples (i.e. mixtures of pennate and centric frustules), masking any potential differences between planktonic and benthic Si cycling. Conspicuously, there are high amplitude variations in the BSi flux. A maximum in BSi accumulation during the 1940–60s (37.5% or 0.42 g cm^{-2} a^{-1} BSi flux) (Fig. 7) is probably triggered by additional nitrogen inputs, as indicated by enhanced *Artemisia* pollen during that period described by Theuerkauf et al. (2015). The abrupt decline in BSi contents during the 1980s to 10% (~0.1 g cm^{-2} a^{-1} BSi flux) might be linked to other planktonic groups outcompeting diatoms, which are limited by Si availability as found in a number of other freshwater systems (e.g. Kemp et al., 2005; Schelske et al., 1983). Advanced eutrophication and limited Si availability are also the most likely explanations for declining frustule sizes during the last 60 years. Increased nutrient concentrations in Tiefer See favoring vegetative proliferation of diatom cells, result in smaller frustule sizes as shown e.g. for the Chesapeake Bay (Cooper, 1995). Smaller frustule sizes again would favor BSi re-dissolution in the water column or the uppermost sediment.

A higher resolution $\delta^{30}Si_{diatom}$ record of the last 150 years would be necessary to analyze the importance of the catchment development and human activity in the modern ecosystem. Typically, small diatom frustules (<40 μm), hinder the separation of sufficient material for isotope measurements by our hand-picking protocol. However, if we consider the ASi pool in the catchment soils to be depleted, and the connection to Flacher See reduced due to lower lake levels in the last 200 years, the BSi production would predominantly depend on Si recycling within the lake.

6. Conclusions

Lake sediments, and in particular varved sediments, have a great potential for recording changes in terrestrial Si cycling. Our results from Tiefer See, northeastern Germany, show systematic changes linked to climate variations and human activity causing vegetation shifts in the catchment. Our data suggest DSi export from soil pools in disturbed environments to be the dominant control on the local Si budget. DSi input-rates are linked to vegetation changes and influence the $\delta^{30}Si_{DSi}$ whereas diatom production (BSi flux) depends on nutrient inputs and food-web composition (competition for nutrients). The modern system since ca 150 a BP seems to depend on interconnected processes: increasing temperatures, eutrophication, and intensified land use cause short-term changes in water circulation and nutrient inputs. Lake internal processes are probably more important for the modern Si budget of the lake. However, further investigations with higher data resolution would be required here.

Overall, the changes in our $\delta^{30}Si_{diatom}$ record from Tiefer See sediments are caused by a variation of inputs and can be linked to a conceptual model describing soil disturbance periods from a forested catchment, via an early-deforested landscape, to an intensely cultivated ecosystem influencing continental Si cycling (Struyf et al., 2010). Initially, changes in Si cycling at the vegetation-soil interface associated with deforestation and low intensity agriculture lead to a lowering of the $\delta^{30}Si_{DSi}$ supplied into the lake. The intensification of agriculture with increased removal of light ^{28}Si from the catchment as a result of harvesting crops adjusted the terrestrial Si isotope budget and as a consequence diatom $\delta^{30}Si$ increased around 750 a BP. Overall, our data provide longer-term empirical support for the concept of human-induced changes to terrestrial Si cycling via land use change, crop harvesting, and fertilizer usage.

Author contributions

Carla K.M. Nantke – Study concept, sampling, Si isotope and BSi measurements, data discussion, leading manuscript writing. Achim Brauer – Provided sediment samples from Tiefer See, substantially contributed to the data discussion and the writing of the final version of the manuscript. Patrick J. Frings – Study concept, Si isotope measurements, substantially contributed to the data discussion and the writing of the final version of the manuscript. Markus Czymzik – Substantially contributed to the data discussion and the writing of the final version of the manuscript. Thomas Hübener – Diatom taxonomy, substantially contributed to the data

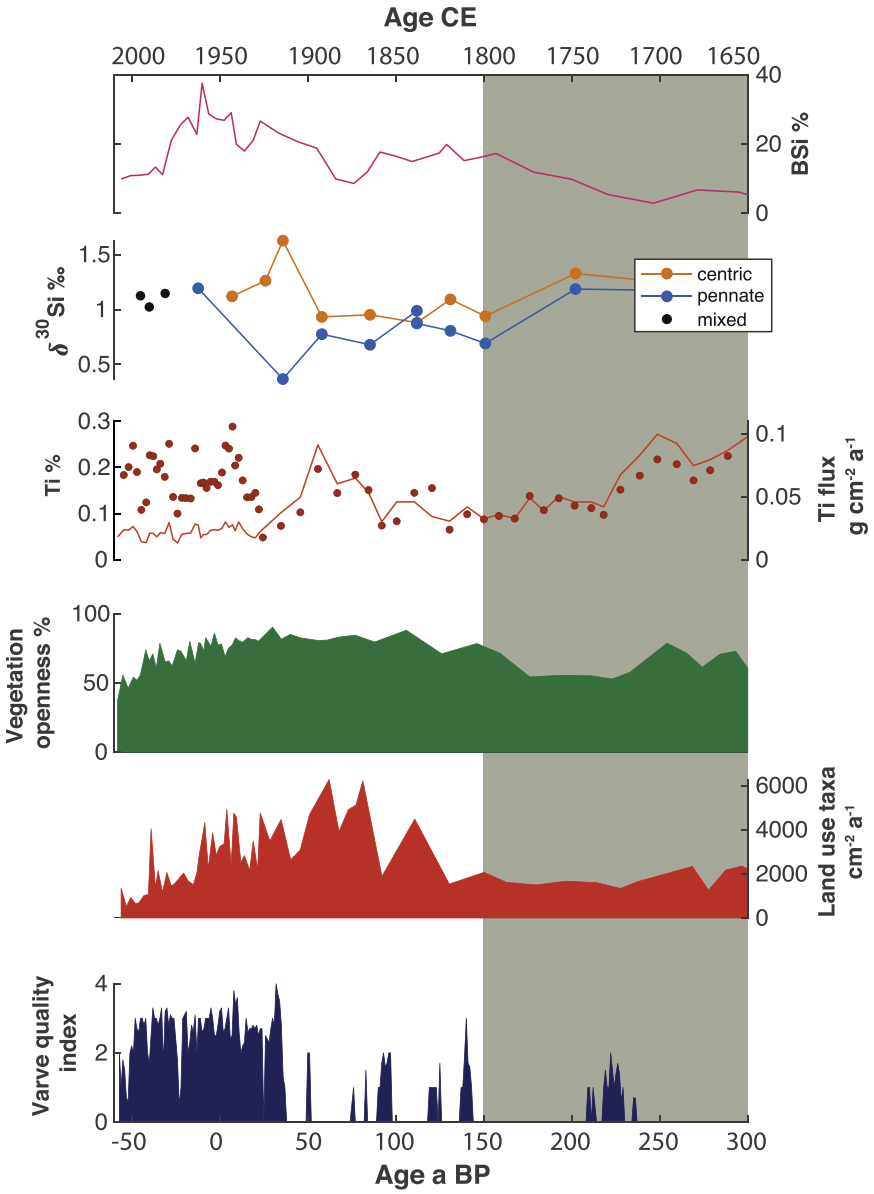

Fig. 7. BSi content %, $\delta^{30}Si_{diatom}$ (centric (orange dots), pennate (blue dots), mixed diatoms (black dots), titanium % and flux (dots), vegetation openness %, land use pollen $cm^{-2}\ a^{-1}$ (comprising *Rumex*, *Secale* and *Cerealia*) showing land cultivation in the catchment and varve quality index (VQI) plotted for the last 360 years. Units III and IV are highlighted by alternating grey and white shaded areas. (For interpretation of the references to colour in this figure legend, the reader is referred to the Web version of this article.)

discussion and the writing of the final version of the manuscript. Johanna Stadmark – Substantially contributed to the data discussion and the writing of the final version of the manuscript. Olaf Dellwig – Element measurements with ICP-OES, substantially contributed to the data discussion and the writing of the final version of the manuscript. Patricia Roeser – Sample preparation for ICP-OES, substantially contributed to the data discussion and the writing of the final version of the manuscript. Daniel J. Conley – Substantially contributed to the data discussion and the writing of the final version of the manuscript.

Declaration of competing interest

The authors declare that they have no known competing financial interests or personal relationships that could have appeared to influence the work reported in this paper.

Acknowledgments

Special thanks go to Sylvia Pinkerneil and Brian Brademann for conducting the monitoring at Tiefer See and help with the water sampling during 2019. Also, we thank Franziska M. Stamm who helped with picking diatom frustules for isotope measurements. Anne Köhler is thanked for support during acid digestions and ICP-OES measurements. This research was supported by the Swedish Research Council (D.J. Conley) and the Royal Physiographic Society in Lund (C.K.M. Nantke), and the Leibniz Association through grant SAW-2017-IOW-2649 (BaltRap). This study used infrastructure of the TERrestrial ENvironmental Observatory (TERENO) NE Germany of the Helmholtz Association. The raw data of this article are available in the PANGAEA data library.

Appendix A. Supplementary data

Supplementary data to this article can be found online at https://doi.org/10.1016/j.quascirev.2021.106869.

References

Alleman, L.Y., Cardinal, D., Cocquyt, C., Plisnier, P., Descy, J., Kimirei, I., Sinyinza, D., André, L., 2005. Silicon isotopic fractionation in lake Tanganyika and its main tributaries. J. Great Lake. Res. 31, 509–519. https://doi.org/10.1016/S0380-1330(05)70280-X.

Barão, L., Vandevenne, F., Clymans, W., Frings, P.J., Ragueneau, O., Meire, P., Conley, D.J., Struyf, E., 2015. Alkaline-extractable silicon from land to ocean: a challenge for biogenic silicon determination. Limnol Oceanogr. Methods 13, 329–344. https://doi.org/10.1002/lom3.10028.

Battarbee, R.W., Kneen, M.J., 1982. The use of electronically counted microspheres in absolute diatom analysis. Limnol. Oceanogr. 27, 184–188. https://doi.org/10.4319/lo.1982.27.1.0184.

Bidle, K.D., Brzezinski, M.A., Long, R.A., Jones, J.L., Azam, F., 2003. Diminished efficiency in the oceanic silica pump caused by bacteria-mediated silica dissolution. Limnol. Oceanogr. 48, 1855–1868. https://doi.org/10.4319/lo.2003.48.5.1855.

Bradshaw, E.G., Rasmussen, P., Nielsen, H., Anderson, N.J., 2005. Mid- to late-Holocene land-use change and lake development at Dallund Sø, Denmark: trends in lake primary production as reflected by algal and macrophyte remains. Holocene 15, 1130–1142. https://doi.org/10.1191/0959683605hl885rp.

Cardinal, D., Alleman, L.Y., de Jong, J., Ziegler, K., André, L., 2003. Isotopic composition of silicon measured by multicollector plasma source mass spectrometry in dry plasma mode. J. Anal. At. Spectrom. 18, 213–218. https://doi.org/10.1039/b210109b.

Closset, I., Cardinal, D., Bray, S.G., Thil, F., Djouraev, I., Rigual-hernández, A.S., Trull, T.W., 2015. Seasonal variations, origin, and fate of settling diatoms. Global Biogeochem. Cycles 29, 1495–1510. https://doi.org/10.1002/2015GB005180.

Clymans, W., Struyf, E., Govers, G., Vandevenne, F., Conley, D.J., 2011. Anthropogenic impact on amorphous silica pools in temperate soils. Biogeosciences 8, 2281–2293. https://doi.org/10.5194/bg-8-2281-2011.

Cockerton, H.E., Street-Perrott, F.A., Barker, P.A., Leng, M.J., Sloane, H.J., Ficken, K.J., 2015. Orbital forcing of glacial/interglacial variations in chemical weathering and silicon cycling within the upper White Nile basin, East Africa: stable-isotope and biomarker evidence from Lakes Victoria and Edward. Quat. Sci. Rev. 130, 57–71. https://doi.org/10.1016/j.quascirev.2015.07.028.

Conley, D.J., 1998. An interlaboratory comparison for the measurement of biogenic silica in sediments. Mar. Chem. 63, 39–48.

Conley, D.J., Likens, G.E., Buso, D.C., Saccone, L., Bailey, S.W., Johnson, C.E., 2008. Deforestation causes increased dissolved silicate losses in the Hubbard Brook Experimental Forest. Global Change Biol. 14, 2548–2554. https://doi.org/10.1111/j.1365-2486.2008.01667.x.

Conley, D.J., Schelske, C.L., 2001. Biogenic silica. In: Smol, J.P., Birks, H.J.B., Last, W.M. (Eds.), Tracking Environmental Change Using Lake Sediments. Terrestrial, Algal, and Siliceous Indicators. Kluwer, Dordrecht, pp. 281–293.

Cooke, J., DeGabriel, J.L., Hartley, S.E., 2016. The functional ecology of plant silicon: geoscience to genes. Funct. Ecol. 30, 1270–1276. https://doi.org/10.1111/1365-2435.12711.

Cooper, S.R., 1995. Chesapeake Bay watershed historical land use: impact on water quality and diatom communities. Ecol. Appl. 5, 703–723. https://doi.org/10.2307/1941979.

Cornelis, J.T., Delvaux, B., 2016. Soil processes drive the biological silicon feedback loop. Funct. Ecol. 30, 1298–1310. https://doi.org/10.1111/1365-2435.12704.

Cornelis, J.T., Delvaux, B., Georg, R.B., Lucas, Y., Ranger, J., Opfergelt, S., 2011. Tracing the origin of dissolved silicon transferred from various soil-plant systems towards rivers: a review. Biogeosciences 8, 89–112. https://doi.org/10.5194/bg-8-89-2011.

Cornelis, J.T., Weis, D., Lavkulich, L., Vermeire, M.L., Delvaux, B., Barling, J., 2014. Silicon isotopes record dissolution and re-precipitation of pedogenic clay minerals in a podzolic soil chronosequence. Geoderma 235–236, 19–29. https://doi.org/10.1016/j.geoderma.2014.06.023.

Czymzik, M., Muscheler, R., Brauer, A., Adolphi, F., Ott, F., Kienel, U., Dräger, N., Słowiński, M., Aldahan, A., Possnert, G., 2015. Solar cycles and depositional processes in annual 10Be from two varved lake sediment records. Earth Planet Sci. Lett. 428, 44–51. https://doi.org/10.1016/j.epsl.2015.07.037.

De la Rocha, C.L., Brzezinski, M.A., DeNiro, M.J., 1997. Fractionation of silicon isotopes by marine diatoms during biogenic silica formation. Geochem. Cosmochim. Acta 61, 5051–5056. https://doi.org/10.1016/S0016-7037(97)00300-1.

Dellwig, O., Wegwerth, A., Schnetger, B., Schulz, H., Arz, H.W., 2019. Dissimilar behaviors of the geochemical twins W and Mo in hypoxic-euxinic marine basins. Earth Sci. Rev. 193, 1–23. https://doi.org/10.1016/j.earscirev.2019.03.017.

DeMaster, D.J., 1981. The supply and accumulation of silicon in the marine environment. Geochemica Cosmochim 45, 1715–1732. https://doi.org/10.1016/0016-7037(81)90006-5.

Dräger, N., Plessen, B., Kienel, U., Słowiński, M., Ramisch, A., Tjallingii, R., Pinkerneil, S., Brauer, A., 2019. Hypolimnetic oxygen conditions influence varve preservation and δ13C of sediment organic matter in Lake Tiefer See, NE Germany. J. Paleolimnol. 62, 181–194. https://doi.org/10.1007/s10933-019-00084-2.

Dräger, N., Theuerkauf, M., Szeroczyńska, K., Wulf, S., Tjallingii, R., Plessen, B., Kienel, U., Brauer, A., 2017. Varve microfacies and varve preservation record of climate change and human impact for the last 6000 years at Lake Tiefer See (NE Germany). Holocene 27, 450–464. https://doi.org/10.1177/0959683616660173.

Dürr, H.H., Meybeck, M., Hartmann, J., Laruelle, G.G., Roubeix, V., 2011. Global spatial distribution of natural riverine silica inputs to the coastal zone. Biogeosciences 8, 597–620. https://doi.org/10.5194/bg-8-597-2011.

Eggimann, D.W., Manheim, F.T., Betzer, P.R., 1980. Dissolution and analysis of amorphous silica in marine sediments. J. Sediment. Petrol. 50, 215–225. https://doi.org/10.1306/212F79AF-2B24-11D7-8648000102C1865D.

Frick, D., Remus, R., Sommer, M., Augustin, J., von Blanckenburg, F., 2020. Silicon isotope fractionation and uptake dynamics of three crop plants: laboratory studies with transient silicon concentrations. Biogeosci. Discuss. 1–26. https://doi.org/10.5194/bg-2020-66.

Frings, P., 2017. Revisiting the dissolution of biogenic Si in marine sediments: a key term in the ocean Si budget. Acta Geochim 36, 429–432. https://doi.org/10.1007/s11631-017-0183-1.

Frings, P.J., Clymans, W., Fontorbe, G., Rocha, C.L.D. La, Conley, D.J., 2016. The continental Si cycle and its impact on the ocean Si isotope budget. Chem. Geol. 425, 12–36. https://doi.org/10.1016/j.chemgeo.2016.01.020.

Geilert, S., Grasse, P., Doering, K., Wallmann, K., Ehlert, C., Scholz, F., Frank, M., Schmidt, M., Hensen, C., 2020. Impact of ambient conditions on the Si isotope fractionation in marine pore fluids during early diagenesis. Biogeosciences 17, 1745–1763. https://doi.org/10.5194/bg-17-1745-2020.

Georg, R.B., Reynolds, B.C., Frank, M., Halliday, A.N., 2006. New sample preparation techniques for the determination of Si isotopic compositions using MC-ICPMS. Chem. Geol. 235, 95–104. https://doi.org/10.1016/j.chemgeo.2006.06.006.

Heathcote, A.J., Ramstack Hobbs, J.M., Anderson, N.J., Frings, P.J., Engstrom, D.R., Downing, J.A., 2014. Diatom floristic change and lake paleoproduction as evidence of recent eutrophication in shallow lakes of the midwestern USA. J. Paleolimnol. 53, 17–34. https://doi.org/10.1007/s10933-014-9804-4.

Houk, V., Klee, R., Tanaka, H., 2014. Atlas of freshwater centric diatoms with a brief key and descriptions. Part IV. Stephanodiscaceae B: Stephanodiscus, cyclostephanos, pliocaenicus, hemistephanos, Stephanocostis,Mesodictyon & spicaticribra. Fottea 14, 1–530.

Houk, V., Klee, R., Tanaka, H., 2010. Atlas of freshwater centric diatoms with a brief key and descriptions, Part III. Stephanodiscaceae A: Cyclotella, Tertiarius, Discostella. Fottea 10, 1–498.

Jansen, N., Hartmann, J., Lauerwald, R., Dürr, H.H., Kempe, S., Loos, S., Middelkoop, H., 2010. Dissolved silica mobilization in the conterminous USA. Chem. Geol. 270, 90–109. https://doi.org/10.1016/j.chemgeo.2009.11.008.

Kalbe, L., Werner, H., 1974. Das Sediment des Kummerower Sees. Untersuchungen des Chemismus und der Diatomeenflora. Int. Rev. der gesamten Hydrobiol. und Hydrogr. 59, 755–782. https://doi.org/10.1002/iroh.19740590603.

Kappler, C., Kaiser, K., Tanski, P., Klos, F., Fülling, A., Mrotzek, A., Sommer, M., Bens, O., 2018. Stratigraphy and age of colluvial deposits indicating Late Holocene soil erosion in northeastern Germany. Catena 170, 224–245.

Kemp, W.M., Boynton, W.R., Adolf, J.E., Boesch, D.F., Boicourt, W.C., Brush, G., Cornwell, J.C., Fisher, T.R., Glibert, P.M., Hagy, J.D., Harding, L.W., Houde, E.D., Kimmel, D.G., Miller, W.D., Newell, R.I.E., Roman, M.R., Smith, E.M., Stevenson, J.C., 2005. Eutrophication of Chesapeake Bay: historical trends and ecological interactions. Mar. Ecol. Prog. Ser. 303, 1–29. https://doi.org/10.3354/meps303001.

Kienel, U., Dulski, P., Ott, F., Lorenz, S., Brauer, A., 2013. Recently induced anoxia leading to the preservation of seasonal laminae in two NE-German lakes. J. Paleolimnol. 50, 535–544. https://doi.org/10.1007/s10933-013-9745-3.

Kienel, U., Kirillin, G., Brademann, B., Plessen, B., Lampe, R., Brauer, A., 2017. Effects of spring warming and mixing duration on diatom deposition in deep Tiefer See, NE Germany. J. Paleolimnol. 57, 37–49. https://doi.org/10.1007/s10933-016-9925-z.

Krammer, K., 2003. Cymbopleura, Delicata, Navicymbula, Gophocymbelloides, Afrocymbella. Diatoms of Europe 4. A.R.G. Gantner Verlag, Ruggell.

Krammer, K., 2002. Cymbella. Diatoms of Europe 3. A.R.G. Gantner Verlag, Ruggell.

Krammer, K., 2000. The Genus Pinnularia. Diatoms of Europe 1. A.R.G. Gantner Verlag, Ruggell.

Krammer, K., 1997a. Die cymbelloiden Diatomeen. Eine Monographie der weltweit bekannten Taxa. Teil 1: allgemeines und Encyonema. Bibl. Diatomol. 36, 1–382.

Krammer, K., 1997b. Die cymbelloiden Diatomeen. Eine Monographie der weltweit bekannten Taxa. Teil 2: encyonema part., Encyonopsis and Cymbellopsis. Bibl. Diatomol. 37, 1–469.

Krammer, K., Lange-Bertalot, H., 1988. Bacillariophyceae 2. In: Ettl, H., Gerloff, J., Heynig, H., Mollenhauer, D. (Eds.), Süßwasserflora von Mitteleuropa. VEB Gustav Fischer Verlag, Jena, pp. 1–596.

Lange-Bertalot, H., Moser, G., 1994. Brachysira, monographie der Gattung. Bibl. Diatomol. 29, 1–212.

Levkov, Z., 2009. Amphora Sensu Lato. Diatoms of Europe 5. A.R.G. Gantner Verlag.

Li, Z., Cornelis, J.T., Linden, C. Vander, Van Ranst, E., Delvaux, B., 2020. Neoformed aluminosilicate and phytogenic silica are competitive sinks in the silicon soil–plant cycle. Geoderma 368, 114308. https://doi.org/10.1016/j.geoderma.2020.114308.

Loucaides, S., Van Cappellen, P., Behrends, T., 2008. Dissolution of biogenic silica from land to ocean: role of salinity and pH. Limnol. Oceanogr. 53, 1614–1621. https://doi.org/10.4319/lo.2008.53.4.1614.

Mann, M.E., Zhang, Z., Rutherford, S., Bradley, R.S., Hughes, M.K., Shindell, D.,

Ammann, C., Faluvegi, G., Ni, F., 2009. Global signatures and dynamical origins of the Little ice age and medieval climate anomaly. Science 84 326, 1256–1260. https://doi.org/10.1126/science.1166349.
Morley, D.W., Leng, M.J., Mackay, A.W., Sloane, H.J., Rioual, P., Battarbee, R.W., 2004. Cleaning of lake sediment samples for diatom oxygen isotope analysis. J. Paleolimnol. 31, 391–401. https://doi.org/10.1023/B:JOPL.0000021854.70714.6b.
Nantke, C.K.M., Frings, P.J., Stadmark, J., Czymzik, M., Conley, D.J., 2019. Si cycling in transition zones: a study of Si isotopes and biogenic silica accumulation in the Chesapeake Bay through the Holocene. Biogeochemistry 146, 145–170. https://doi.org/10.1007/s10533-019-00613-1.
Oelze, M., Schuessler, J.A., Blanckenburg, F. Von, 2016. Mass bias stabilization by Mg doping for Si stable isotope analysis by MC-ICP-MS. J. Anal. At. Spectrom. 31, 2094–2100. https://doi.org/10.1039/C6JA00218H.
Opfergelt, S., Georg, R.B., Delvaux, B., Cabidoche, Y.M., Burton, K.W., Halliday, A.N., 2012. Silicon isotopes and the tracing of desilication in volcanic soil weathering sequences. Guadeloupe. Chem. Geol. 326–327, 113–122. https://doi.org/10.1016/j.chemgeo.2012.07.032.
Panizzo, V.N., Swann, G.E.A., MacKay, A.W., Vologina, E., Sturm, M., Pashley, V., Horstwood, M.S.A., 2015. Insights into the transfer of silicon isotopes into the sediment record. Biogeosci. Discuss. 12, 9369–9391. https://doi.org/10.5194/bgd-12-9369-2015.
Reynolds, B.C., Aggarwal, J., André, L., Baxter, D., Beucher, C., Brzezinski, M.A., Engström, E., Georg, R.B., Land, M., Leng, M.J., Opfergelt, S., Rodushkin, I., Sloane, H.J., van den Boorn, S.H.J.M., Vroon, P.Z., Cardinal, D., 2007. An inter-laboratory comparison of Si isotope reference materials. J. Anal. At. Spectrom. 22, 561–568. https://doi.org/10.1039/B616755A.
Roeser, P., Dräger, N., Brykała, D., Ott, F., Pinkerneil, S., Gierszewski, P., Lindemann, C., Plessen, B., Brademann, B., Kaszubski, M., Fojutowski, M., Schwab, M.J., Słowiński, M., Błaszkiewicz, M., Brauer, A., 2021. Advances in understanding calcite varve formation: new insights from a dual lake monitoring approach in the southern Baltic lowlands. Boreas. https://doi.org/10.1111/bor.12506, 0300-9483.
Sauer, D., Saccone, L., Conley, D.J., Herrmann, L., Sommer, M., 2006. Review of methodologies for extracting plant-available and amorphous Si from soils and aquatic sediments. Biogeochemistry 80, 89–108. https://doi.org/10.1007/s10533-005-5879-3.
Schelske, C.L., Stoermer, E.F., Conley, D.J., Robbins, J.A., Glover, R.M., 1983. Early eutrophication in the lower great lakes. Science 84 222, 320–322. https://doi.org/10.1126/science.222.4621.320.
Selig, U., Leipe, T., Dörfler, W., 2007. Paleolimnological records of nutrient and metal profiles in prehistoric, historic and modern sediments of three lakes in Northeastern Germany. Water. Air. Soil Pollut 184, 183–194. https://doi.org/10.1007/s11270-007-9407-z.
Street-Perrott, F.A., Barker, P.A., Leng, M.J., Sloane, H.J., Wooller, M.J., Ficken, K.J., Swain, D.L., 2008. Towards an understanding of late Quatrnary variations in the continental biogeochemical cycle of silicon: multi-isotope and sediment-flux data for lake Rutundu, Mt Kenya, East Africa, since 38 ka BP. J. Quat. Sci. 23, 375–387. https://doi.org/10.1002/jqs.
Strickland, J.D.H., Parsons, T.R., 1972. A Practical Handbook of Seawater Analysis, second ed. Fisheries Research Board of Canada, Ottawa.
Struyf, E., Conley, D.J., 2011. Emerging understanding of the ecosystem silica filter. Biogeochemistry 107, 9–18. https://doi.org/10.1007/s10533-011-9590-2.
Struyf, E., Smis, A., Van Damme, S., Garnier, J., Govers, G., Van Wesemael, B., Conley, D.J., Batelaan, O., Frot, E., Clymans, W., Vandevenne, F., Lancelot, C., Goos, P., Meire, P., 2010. Historical land use change has lowered terrestrial silica mobilization. Nat. Commun. 129, 1–7. https://doi.org/10.1038/ncomms1128.
Swann, G.E.A., Leng, M.J., Juschus, O., Melles, M., Brigham-Grette, J., Sloane, H.J., 2010. A combined oxygen and silicon diatom isotope record of Late Quaternary change in Lake El'gygytgyn, North East Siberia. Quat. Sci. Rev. 29, 774–786. https://doi.org/10.1016/j.quascirev.2009.11.024.
Swann, G.E.A., Panizzo, V.N., Piccolroaz, S., Pashley, V., Horstwood, M.S.A., 2020. Changing nutrient cycling in Lake Baikal , the world ' s oldest lake. Proc. Natl. Acad. Sci. U. S. A. https://doi.org/10.1073/pnas.2013181117.
Theuerkauf, M., Dräger, N., Kienel, U., Kuparinen, A., Brauer, A., 2015. Effects of changes in land management practices on pollen productivity of open vegetation during the last century derived from varved lake sediments. Holocene 25, 733–744. https://doi.org/10.1177/0959683614567881.
Tye, A.M., Kemp, S.J., Poulton, P.R., 2009. Responses of soil clay mineralogy in the Rothamsted Classical Experiments in relation to management practice and changing land use. Geoderma 153, 136–146. https://doi.org/10.1016/j.geoderma.2009.07.019.
Vandevenne, F., Struyf, E., Clymans, W., Meire, P., 2012. Agricultural silica harvest : have humans created a new loop in the global silica cycle? Responsive Community 10, 243–248. https://doi.org/10.1890/110046.
Vandevenne, F.I., Delvaux, C., Hughes, H.J., Andre, L., Ronchi, B., Clymans, W., Cornelis, J., Govers, G., Meire, P., Struyf, E., 2015. Landscape cultivation alters δ30Si signature in terrestrial ecosystems. Sci. Rep. 5 https://doi.org/10.1038/srep07732 https://doi.org/10.1038/srep07732.
Walker, J.C.G., Hays, P.B., Kasting, J.F., 1981. A negative feedback mechanism for the long-term stabilization of earth's surface temperature. J. Geophys. Res. 86, 9776–9782. https://doi.org/10.1029/JC086iC10p09776.
Wieckowska, M., Dörfler, W., Kirleis, W., 2012. Vegetation and settlement history of the past 9000 years as recorded by lake deposits from Großer Eutiner See (Northern Germany). Rev. Palaeobot. Palynol. 174, 79–90. https://doi.org/10.1016/j.revpalbo.2012.01.003.
Williams, L.A., Crerar, D.A., 1985. Silica diagenesis, general mechanisms. J. Sediment. Petrol. 55, 312–321. https://doi.org/10.1306/212F86B1-2B24-11D7-8648000102C1865D.
Wulf, S., Dräger, N., Ott, F., Serb, J., Appelt, O., Gudmundsdóttir, E., van den Bogaard, C., Słowiński, M., Błaszkiewicz, M., Brauer, A., 2016. Holocene tephrostratigraphy of varved sediment records from lakes tiefer see (NE Germany) and czechowskie (N Poland). Quat. Sci. Rev. 132, 1–14. https://doi.org/10.1016/j.quascirev.2015.11.007.